Available online at www.sciencedirect.com
SCIENCE DIRECT®
Journal of Nuclear Materials 329–333 (2004) 518–523
journal of nuclear materials
www.elsevier.com/locate/jnucmat

Study of helium bubble formation in SiCf/PyC/β-SiC composites by dual-beam irradiation

T.S. Duh [a], K.M. Yin [b], J.Y. Yan [b], P.C. Fang [b], C.W. Chen [b], J.J. Kai [b,*], F.R. Chen [b], Y. Katoh [c], A. Kohyama [c]

[a] *Institute of Nuclear Energy Research, Lung-tan, Tau-yuan 325, Taiwan, ROC*
[b] *Center for Electron Microscopy, Department of Engineering and System Science, Nation Tsing-Hua University, 101, Section II, Kuang-fu Road, Hsinchu 300, Taiwan, ROC*
[c] *Institute of Advanced Energy, Kyoto University, Uji, Kyoto 611-0011, Japan*

Abstract

The formation of helium bubbles in the advanced SiC composites, Tyranno-SA SiC/PyC/β-SiC (TSA) and Hi-Nicalon Type-S SiC/PyC/β-SiC (HNS), implanted with helium and irradiated by dual-beam was investigated. Post-implantation annealing was carried out at 1000/1200/1400 °C, and dual-beam irradiation at 800/1000 °C. For He implantation, helium bubbles were observed only in the SiC matrix for annealing temperatures $\geqslant$ 1200 °C. For dual-beam irradiation, no He bubbles were observed for a dose of 10 dpa, but for doses up to 100 dpa, He bubbles were observed in the matrix. Under these irradiation conditions, the TSA and HNS fibers exhibited good microstructural stability against helium influence. In addition, possible diffusion modes were suggested here to describe the diffusion behavior of helium in SiC in different temperature regions.

1. Introduction

SiC composites, due to their good heat resistance and low activation under high energy neutron irradiation, are being considered as structural materials in some future fusion reactor designs. In a fusion reactor, helium and hydrogen may be produced in SiC in the first wall by transmutation reactions during 14 MeV neutron irradiation. He and H production in SiC exposed to 14 MeV neutrons may be approximately 2000 and 800 appm/MW a/m^2 in the first wall region [1]. Hence, SiC in the first wall will be subjected to high neutron irradiation, as well as helium and hydrogen transmutation atoms.

Helium may cause significant swelling in SiC due to its limited diffusivity and insolubility in SiC. In turn, the mechanical properties of SiC composite may be degraded. Therefore, for SiC to be used in a future fusion reactor the formation of helium bubbles in SiC composites under neutron irradiation need to be investigated. Several past studies (e.g., He-retention [2] and He-release [3], and experiments using single- [4,5], dual- [6,7] and even triple-beam [8] irradiations to simulate the fusion reactor environment) have been carried out to investigate the behavior of helium in SiC. All of these studies provided useful information about helium bubble formation and behavior in SiC. However, the helium diffusion mode in SiC has not been clarified. The purpose of this work is to investigate the formation of helium bubbles in SiC by helium implantation and dual-beam irradiation, and then to suggest possible diffusion modes to describe the diffusion behavior of helium in SiC in different temperature regions.

2. Experimental

Two types of advanced SiC composites Tyranno-SA SiC/PyC/β-SiC (TSA) and Hi-Nicalon Type-S SiC/PyC/

* Corresponding author. Tel.: +886-3 5742855/5715131x4280 or 4209; fax: +886-3 5716770/5720724.
E-mail address: jjkai@ess.nthu.edu.tw (J.J. Kai).

0022-3115/$ - see front matter © 2004 Elsevier B.V. All rights reserved.
doi:10.1016/j.jnucmat.2004.04.218

β-SiC (HNS), supplied by Institute of Advanced Energy of Kyoto University, were used in this study. The TSA composite was made with 0–90° two-dimensional Tyranno-SA SiC fabric (UBE Heavy Industries) coated with a pyrolytic carbon (PyC) layer using a chemical vapor deposition (CVD) process. The fabric layer was then infiltrated with β-SiC using a chemical vapor infiltration (CVI) process. The HNS composite was made with the same materials by similar processes except that the fabric layers were made with −30°/0°/30° two-dimensional Hi-Nicalon Type-S fibers (Nippon Carbon).

Beam bombardment experiments were carried out using the Tandem and Van de Graff Accelerators at Tsing-Hua University. The helium behavior was examined after three types of irradiation tests: He implantation (He^+), single-beam (Si^{3+}) and dual-beam ($Si^{3+} + He^+$) irradiations. The irradiation conditions listed in Table 1 for each composite type were the same. A schematic illustration of the SiC composite under dual-beam irradiation is shown in Fig. 1(a). For He implantation and single-beam irradiation, the direction of the incident beam was perpendicular to the surface of the sample. For the dual-beam irradiation, the incident Si^{3+} beam was normal to the surface and the He^+ beam was 45° away from the normal. The depth distributions for the He concentration and displacement damage in SiC as calculated by the TRIM code are shown in Fig. 2. For dual-beam irradiation, the peak displacement damage in SiC occurred at a depth of about 2.4 μm, and the peak He/dpa ratio and the damage rate values were set about 150 appm/dpa and 1.1×10^{-3} dpa/s, respectively.

After irradiation, TEM specimens were prepared for microstructure observations using a field emission gun transmission electron microscopy (FEGTEM). The irradiated area in the central region of the specimen was

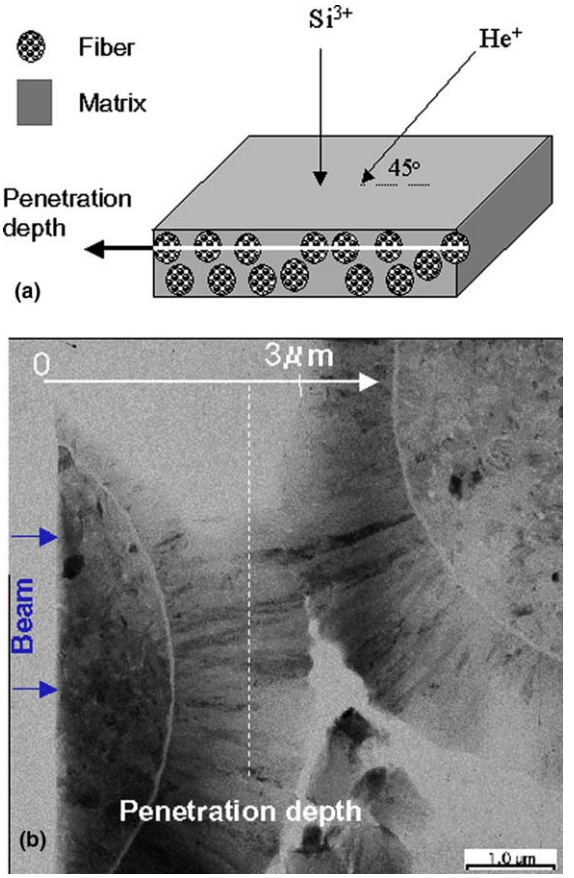

Fig. 1. (a) The schematic illustration of the SiC composite sample under dual-beam irradiation. The peak displacement damage region is marked with a white line, and (b) a typical TEM micrograph in which the He peak displacement damage region can be estimated by the penetration depth of incident particle.

Table 1
The test conditions for Tyranno-SA (TSA) and Hi-Nicalon Type-S (HNS) SiC composites

Test conditions	TSA and HNS composites
He implantation and annealing	Step 1: Implantation with He^+, 2 MeV, 10 000 appm at room temperature Step 2: Annealing at 1000/1200/1400 °C after implantation, each for an hour
Single-beam irradiation	Si^{3+}, 6 MeV, 10 dpa With irradiation temperatures of 800/1000 °C
Dual-beam irradiation	He^+, 1.5 MeV, 1500 appm Si^{3+}, 6 MeV, 10 dpa With irradiation temperatures of 800/1000 °C
	He^+, 1.5 MeV, 15 000 appm Si^{3+}, 6 MeV, 100 dpa With an irradiation temperature of 1000 °C

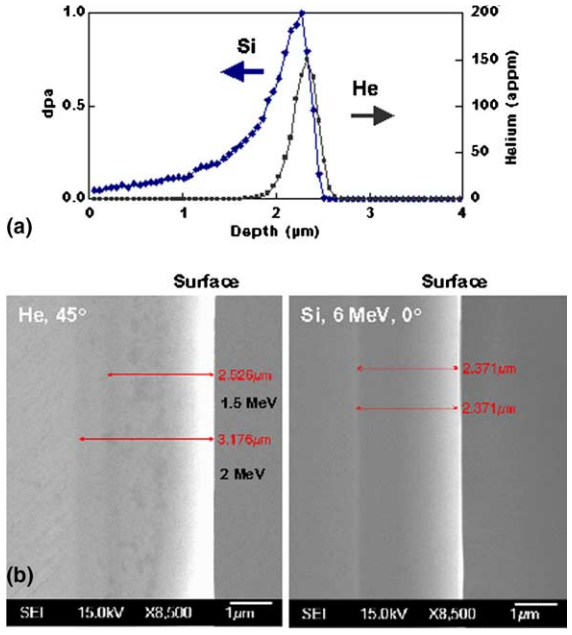

Fig. 2. (a) The depth distributions calculated by the TRIM code for the He concentration and displacement damage in SiC composites, and (b) SEM micrography of the penetration depths of Si (6 MeV) and He (1.5 and 2 MeV, 45° away from the normal) in the SiC composites.

thinned by an ion-miller. A typical TEM micrograph is shown in Fig. 1(b).

3. Results

3.1. Microstructural observations of the as received TSA and HNS composites

A typical TEM micrograph of the TSA composite is shown in Fig. 3(a) and (b). The average diameter of the TSA fibers is 8 μm, the SiC grain size in the fibers is 50–500 nm [9], and the C/Si atomic ratio is close to 1. A small amount of C phase of 10–60 nm size exist between SiC grains in the fibers. The thickness of the applied PyC layer was 50–100 nm.

A typical TEM micrograph of the HNS composite is shown in Fig. 3(c) and (d). The average diameter of the fibers is 14 μm, the SiC grain size is 10–100 nm [9], and the C/Si ratio is also close to 1. A small amount of C phase of about 10–20 nm size exist between SiC grains in the HNS-fibers. The average thickness of the PyC layer is about 80 nm. In both TSA and HNS composites, the SiC matrix is composed of elongated β-SiC grains with an average diameter of 50 nm. The elongated β-SiC matrix grains grew in the radial direction away from the fiber surface.

3.2. Helium implantation

The microstructures of TSA composite implanted with helium and annealed at different temperatures for an hour were observed by TEM. Helium bubbles were observed only in the matrix, not in the fibers, for annealing temperatures $\geqslant 1200$ °C, as shown in Fig. 4(a)–(c). Most of the helium bubbles accumulated along the grain boundaries. The average size of the helium bubbles was 3 nm after annealing at 1200 °C, and 8 nm at 1400 °C. No helium bubbles were observed in the PyC coating layers.

For the HNS composite, the helium bubbles were also observed only in the SiC matrix for annealing temperatures $\geqslant 1200$ °C. No helium bubbles were observed in the PyC coating layers nor in the fibers.

3.3. Single-beam (Si^{3+}) and dual-beam ($Si^{3+} + He^{+}$) irradiations

The microstructures of the TSA and HNS composites, both irradiated with single-beam 6 MeV Si^{3+}-ions up to 10 dpa at irradiation temperatures of 800 and 1000 °C, were investigated by TEM. No irradiation-induced microstructural defects were observed. For the cases of dual-beam ($Si^{3+} + He^{+}$) irradiation of the TSA and HNS composites up to 10 dpa and 1500 appm He at irradiation temperatures of 800 and 1000 °C, no He bubbles were observed in either the fiber or the matrix. Similarly, Nogami et al. [6], for irradiated SiCf/SiC composite up to 10 dpa and 1000 appm He at 800 and 950 °C observed no He bubble formation in the matrix. It can be concluded from these results for single- and dual-beam irradiations at 800–1000 °C, both TSA and HNS composites exhibit good microstructural stability against helium bubble formation for doses up to 10 dpa.

However, for dual-beam irradiation up to 100 dpa and 15 000 appm He at an irradiation temperature of 1000 °C, helium bubbles were found in the matrix, but not in the fiber and PyC coating layer, as shown in Fig. 5.

4. Discussion

These results indicated that (1) if helium bubbles were formed, they formed only in the CVI-SiC-matrix for either composite, but not in the PyC coating layers nor in the fibers, under any of the irradiation conditions examined, and (2) for the dual-beam $Si^{3+} + He^{+}$ irradiation at 1000 °C, helium bubble formation only in the CVI-SiC-matrix occurred when the displacement damage was high (~100 dpa).

The reason for observing no He bubbles in the PyC coating layers may be understood by the high diffusion coefficient of He in carbon. The diffusion coefficient of

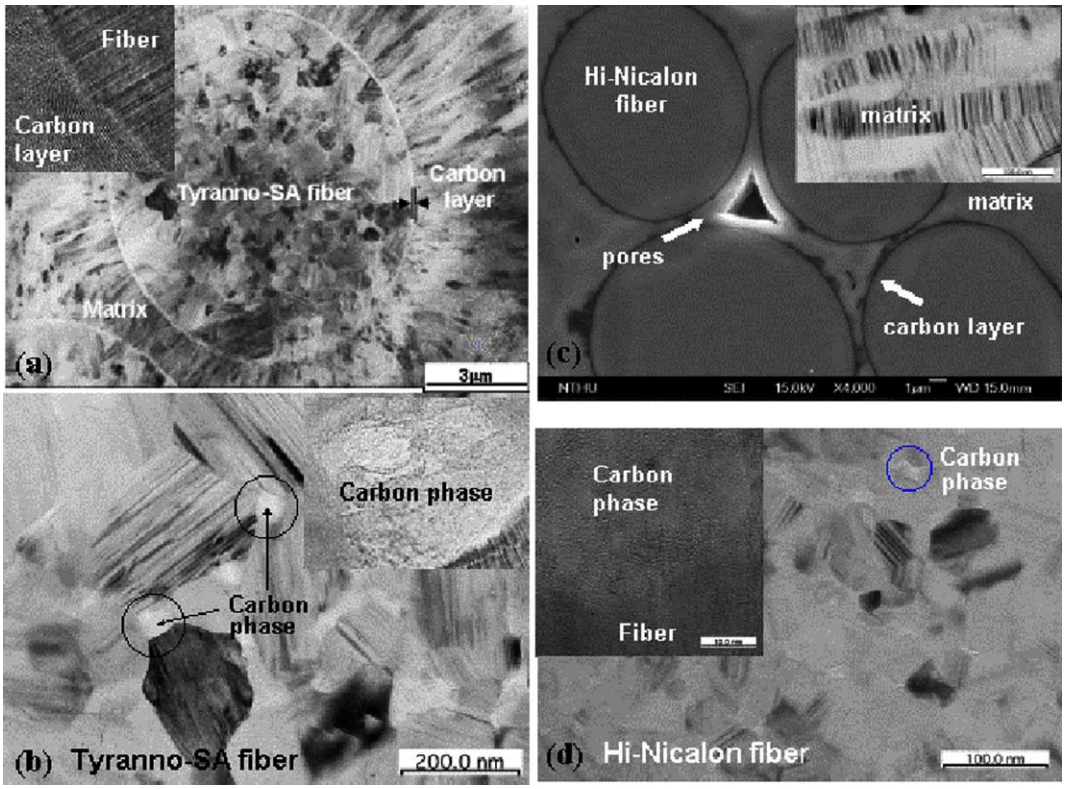

Fig. 3. Typical TEM micrographs of TSA and HNS composites showing: (a) a cross section view of TSA fiber within the composite matrix, and (b) microstructural observations within the TSA fiber region, (c) a cross section view of HNS fiber within the composite matrix and (d) microstructural observations within the HNS fiber region.

He in carbon was about 30 times higher than in SiC at 1000 °C [2], and helium release from carbon layers started below 500 °C [3]. Hence, almost all the implanted He ions in the PyC coating layers were released after the post-implantation annealing, as well as during the dual-beam irradiation at 1000 °C.

Helium release study [3] showed that He release from SiC fiber was observed above 1100 °C, and was increasing with temperatures up to 1400 °C. At 1000 °C, therefore, the implanted He ions should be still remained and trapped somewhere in the fibers. One of the possible trapping sites for He in SiC fiber would be grain boundaries. The grains in crystallized SiC fibers are much smaller than those in the SiC matrix, as displayed in Fig. 3(a). Due to the high grain boundary density, the grain boundaries in the fibers would have enough capacity to keep helium from precipitation [7]. This may explain why helium bubbles were not observed in the fibers under any of the irradiation conditions examined.

Here, we attempt to find the He diffusion modes for different temperature regions so as to understand the helium bubble formation behavior in SiC. The He release studies [3,10] showed that (a) a small amount of helium have released from SiC at temperatures below 500 °C, (b) a large amount of helium are released in the temperature range 800–1500 °C and (c) a final helium release peak shows up and increases very rapidly in the even higher temperature region above 1700 °C. Based on those results of the He release studies, possible He diffusion modes for different temperature regions are suggested and described below.

Due to helium has become mobile for temperatures below 500 °C, the He diffusion in SiC is assumed to be via the hindered interstitial diffusion mode [11], in which helium was assumed to perform a series of interstitial jumps, which were interrupted temporarily by trapping at vacancy-clusters. The trapped helium may dissociate from its trapping site into an interstitial position and go on diffusing. If the binding energy of helium to its trapping site is large, the contribution to the interstitial diffusion from the trapped helium may be ignored. Because helium is easily trapped by vacancy-clusters [8], the helium atoms at interstitial positions are normally much less than those at trapping sites. This can explain why only a small amount helium are released from SiC at temperatures below 500 °C.

In the temperature range 800–1500 °C, helium is assumed to diffuse in SiC via the vacancy mechanism.

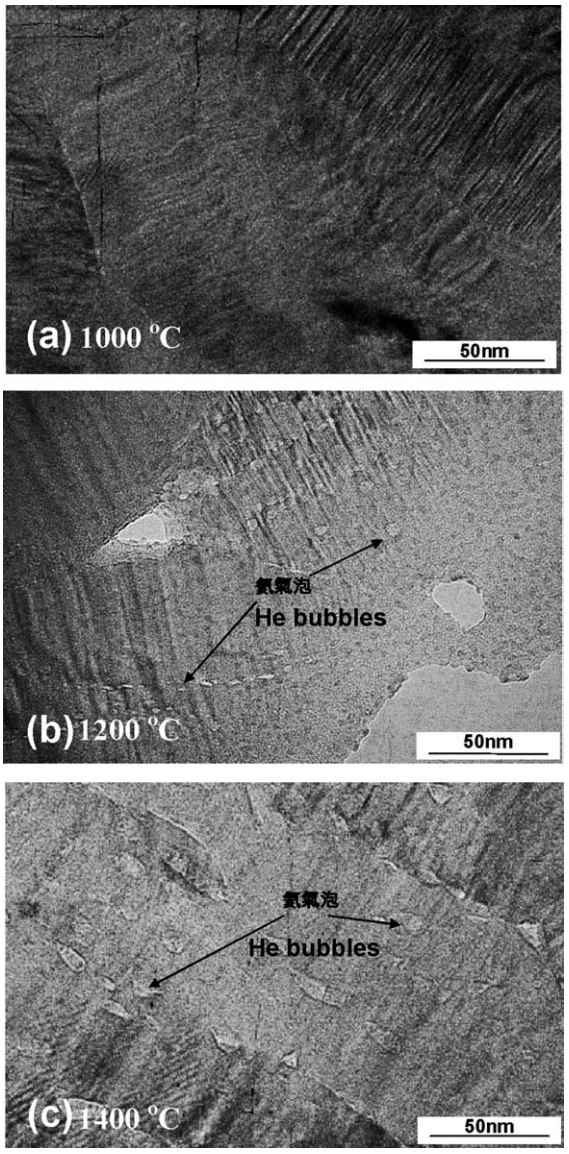

Fig. 4. TEM micrographs of the TSA composite matrix implanted with helium and annealed at temperatures (a) 1000, (b) 1200 and (c) 1400 °C. Helium bubbles were observed only in the SiC matrix, not in the fiber, for annealing temperatures 1200 °C and higher.

Helium atoms and vacancies may form helium–vacancy pairs and move together, due to that most helium are easily trapped by vacancies. Helium can then become mobile through the vacancy motion. In many of electron spin resonance (ESR) [12] and helium release [10] studies on β-SiC, it has been reported that silicon vacancies start substantial migration at about 800 °C. Therefore, for temperatures above 800 °C the He diffusion in SiC grains via vacancy mechanism would be dominant.

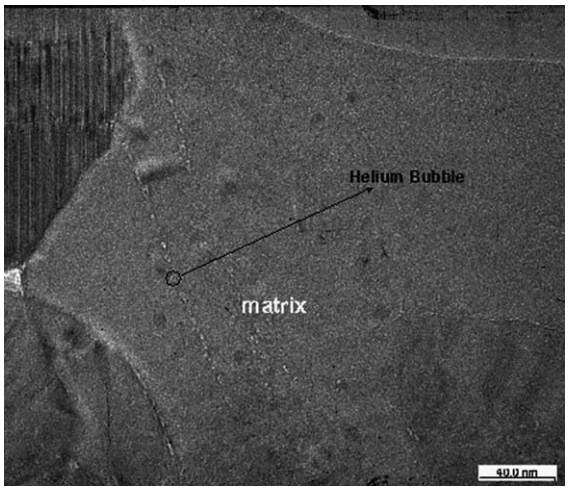

Fig. 5. A TEM micrograph of the TSA composite matrix after dual-beam irradiation up to 100 dpa and 15 000 appm He at an irradiation temperature of 1000 °C. Helium bubbles are found in the matrix, but not in the fiber or the PyC coating.

Moreover, for even higher temperature region above 1700 °C, the dissociation of He from vacancies or vacancy-related defects might become effective, and in that case helium can move by itself. In bulk SiC, the final He release peak is related to the interlinkage of bubbles at grain boundaries to form pores open to the surface [3]. But in SiC powder (with almost no grain boundary in each powder particle), this peak might be related to the dissociation of He from vacancies or vacancy-related defects. After dissociating from vacancies or vacancy-related defects, helium can be released from SiC directly.

During the dual-beam irradiation at 1000 °C, He diffusion in SiC was mainly via the vacancy mechanism. The helium–vacancy pairs would migrate to grain boundaries to form helium bubbles. Under irradiation, the vacancy diffusion may be enhanced, which, in turn, may promote the He migration to grain boundaries. On the other hand, the radiation-introduced defects, such as vacancy-clusters and cavities, may trap the helium in the grain. Therefore, irradiation would not necessarily promote the formation of helium bubble on grain boundary. Under certain conditions, irradiation may suppress the formation of helium bubble in SiC. We can see the suppression effect on the helium diffusion in SiC in this and other dual-beam studies [6]. The dual-beam results of this work (with irradiation conditions: 10 dpa Si^{3+}, 1500 appm He^{+} at 1000 °C) and Nogami (10 dpa C^{2+}, 1000 appm He^{+} at 950 °C) showed no helium bubbles observed in the dual-beam irradiated β-SiC. However, for β-SiC implanted with helium of about the same concentration (~1000 appm) at room temperature and annealing at 1050 °C for 1 h, helium bubbles have already been observed on grain boundaries [1]. On the other hand, for dual-beam irradiation up to 100 dpa and

helium >6000 appm, helium bubbles can be observed at the grain boundaries in β-SiC, as shown in this and Kishimoto studies [7]. In those cases, the trapped He atoms may not increase with doses due to that the radiation-induced defects might have been saturated. Therefore, helium bubbles in β-SiC can be observed for dual-beam irradiation with high doses.

5. Conclusions

In this study, helium bubble formation in advanced TSA and HNS composites was investigated by helium implantation and dual-beam irradiation and possible diffusion modes were suggested here to describe the diffusion behavior of helium in SiC in different temperature regions. The main results are summarized as follows:

(1) After helium implantation at room temperature to a concentration of 10 000 appm, helium bubbles were observed only in the CVI-SiC matrix for post-implantation annealing temperatures $\geqslant 1200$ °C in both composites. No helium bubbles were observed in the PyC coating or the TSA or the HNS fibers.
(2) After dual-beam ($Si^{3+} + He^{+}$) irradiation at 800 and 1000 °C, no He bubbles were observed in the CVI-SiC matrix at doses of 10 dpa. However, for dual-beam irradiation at 1000 °C up to 100 dpa, He bubbles were observed. No helium bubbles were observed in the fibers or the PyC coating for any of the irradiation conditions.
(3) Possible diffusion modes are suggested here to describe the diffusion behavior of He in SiC in different temperature regions.

Acknowledgement

This study is financially supported by the National Science Council, ROC under contract number of NSC-92-2212-E-007-028.

References

[1] L.L. Snead, R.H. Jones, A. Kohyama, P. Fenici, J. Nucl. Mater. 233–237 (1996) 26.
[2] P. Jung, J. Nucl. Mater. 191–194 (1992) 377.
[3] K. Sasaki, T. Yano, T. Maruyama, T. Iseki, J. Nucl. Mater. 179–181 (1991) 407.
[4] A. Hasegawa, B.M. Oliver, S. Nogami, K. Abe, R.H. Jones, J. Nucl. Mater. 283–287 (2000) 811.
[5] A. Hasegawa, M. Saito, S. Nogami, K. Abe, R.H. Jones, H. Takahashi, J. Nucl. Mater. 264 (1999) 355.
[6] S. Nogami, A. Hasegawa, K. Abe, T. Taguchi, R. Yamada, J. Nucl. Mater. 283–287 (2000) 268.
[7] H. Kishimoto, Y. Katoh, A. Kohyama, J. Nucl. Mater. 307–311 (2002) 1130.
[8] T. Taguchi, E. Wakai, N. Igawa, S. Nogami, L.L. Snead, A. Hasegawa, S. Jitsukawa, J. Nucl. Mater. 307–311 (2002) 1135.
[9] A.R. Raffray, R. Jones, G. Aiello, M. Billone, L. Giancarli, H. Golfier, A. Hasegawa, Y. Katoh, A. Kohyama, S. Nishio, B. Riccardi, M.S. Tillack, Fus. Eng. Des. 55 (2001) 55.
[10] Y. Pramono, M. Imai, T. Yano, J. Nucl. Sci. Technol. 40 (7) (2003) 531.
[11] V. Philipps, K. Sonnenberg, J. Nucl. Mater. 107 (1982) 271.
[12] A. Kawasuso, H. Itoh, N. Morishita, M. Yoshikawa, T. Ohshima, I. Nashiyama, S. Okada, H. Okumura, S. Yoshida, Appl. Phys. A 67 (1998) 209.